ACS OMEGA

http://pubs.acs.org/journal/acsodf

Article

Insights into the Structural and Dielectric Behavior of Composites Produced from EPDM Waste Processed through a Devulcanization Method and SBR

Marc Marín-Genescà,* Jordi García-Amorós, Miguel Mudarra, Lluis Massagués Vidal, Javier Cañavate, and Xavier Colom

Cite This: *ACS Omega* 2023, 8, 12830−12841

Read Online

ACCESS | Metrics & More | Article Recommendations

ABSTRACT: Ethylene propylene diene monomer (EPDM) is one of the most used polymers in the world. It is an elastomer, which means that the existing cross-linking between the main chains of the polymer created during the vulcanization process makes its recycling difficult. In this paper, a possible solution to this issue is studied. The devulcanization of EPDM is achieved by a thermomechanical process followed by microwave irradiation. These combined treatments suppress the cross-linking, yielding a material (EPDMd) that can be successfully blended to form composites. A common elastomer, styrene butadiene rubber (SBR), has been selected as the matrix. The new SBR/EPDMd composites can be useful as elastomeric dielectric materials and can contribute to the recycling of the discarded EPDM. To provide a better understanding of their microstructure and its relationship with their micro- and macroscopic behavior, samples containing 20 and 40% of EPDMd have been tested by thermogravimetric and dielectric analysis, focusing on variables such as the thermal properties of the blends, permittivity, electric modulus, conductivity, and activation energies. The results show interesting changes linked to the presence of EPDMd in the SBR matrix, such as the displacement of the β dielectric relaxation toward higher frequencies. The correct integration between the two phases is confirmed by the absence of any Maxwell−Wagner−Sillars type relaxation in their dielectric behavior. The presence of additives in the EPDMd samples has an effect on the conductivity, mainly due to the conductive aluminum silicate present in the EPDMd, which acts toward increasing some key dielectric features like conductivity and permittivity and decreasing the insulation of the final SBR/EPDMd materials. The inclusion of EPDMd also affects the α relaxations (low frequencies) and suppresses the β relaxations (high frequencies). The samples showed a non-Debye dielectric behavior. In short, a compact and well-integrated material with a dielectric behavior is created, which exhibits interesting differences from the reference SBR matrix. Finally, it is concluded that the compounds tested are suitable for applications as electrical insulators.

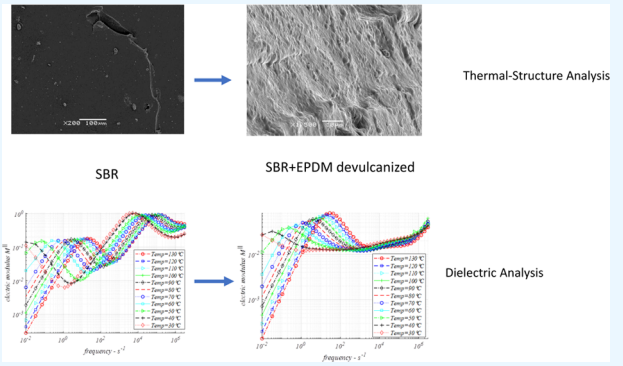

1. INTRODUCTION

Ethylene propylene diene monomer (EPDM) is a very useful type of rubber.[1,2] It is very durable and flexible and therefore has a wide range of applications, especially in the automotive field in manufacturing gasket hoses and sealants but also in domestic uses like waterproofing roofs or nonslip surfaces. EPDM is also impermeable and has interesting mechanical, thermal, and electrical properties.[3,4]

These properties are based on its chemical structure, which is characterized by the absence of double bonds that are responsible for the degradation of many other elastomers and by its cross-linked structure, achieved by the vulcanization process.[5,6] The cross-linked structure, which gives elastomers and thermosets a large part of their interesting features, constitutes a challenge in terms of recycling. Cross-linked materials cannot be melted or dissolved and are, therefore, difficult to integrate in any kind of reprocessing. Expanding the possibilities of recycling these materials at the end of their useful life[7,8] is nowadays an object of intensive research at the international level.[9,10]

The main recycling strategies for industrial rubbers are limited and with low value addition.[11−14] One of them is energy recovery, which is basically waste combustion integrated into processes like cement production. Grinding and mixing with

Received: December 21, 2022
Accepted: February 24, 2023
Published: March 30, 2023

other base or matrix polymers is also proposed to reuse these materials and several studies have designed materials that can also include other residua[15] and are eventually useful in civil applications such as playgrounds, street furniture, or other applications with low requirements, as well as with bituminous mixtures to constitute new materials such as asphalts.

Since the mid-90s, a series of strategies have focused on eliminating the cross-linking of the elastomers produced by the vulcanization process, achieving a material that would be suitable for recycling in a much more useful way. These processes, called devulcanization, have been mainly applied to rubber tires, because they are the most abundant elastomeric subproduct. The reclaiming and devulcanization of elastomers have been studied in depth by several groups.[16] Devulcanization consists in the breaking of the sulfur bridges that cross-link the elastomers, trying to keep the main polymeric chains intact and to regenerate a material that could be integrated in its original application. An example of this strategy has been applied by Colom et al. to EPDM scraps from roofing isolation.[17]

Devulcanization can be achieved by several methods:[18−20] thermomechanical, microwaves irradiation, ultrasounds, and sulfur-oxidizing microorganisms. Today, the most successful methods are thermomechanical[16] and microwaves.[17]

Elastomeric materials are widely used as dielectrics, with their application often being considered in terms of their recycling possibilities. Their dielectric behavior has been well studied and described, especially styrene butadiene rubber (SBR)[21,22] and natural rubber (NR),[23,24] which are the main components of the tires of cars, trucks, and planes. Rubber composites contain in most cases several phases; this heterogeneity causes interfacial polarization, leading to the Maxwell−Wagner−Sillars (MWS) phenomena.[25,26] Other dielectric behaviors depending on the type of material can be described by Debye, Havriliak−Negami, Cole−Cole, or Davidson-Cole interpretations.[27−29]

The most important dielectric relaxations are α, β, γ, and MWS.[30−32] They are commonly found in the frequency range between 0.1 and 3×10^6 Hz. The α relaxations are not associated to Arrhenius behavior and take place at low frequencies. Contrarily, the β relaxations occur at high frequencies and can be associated with Arrhenius-type phenomena or be thermally activated.

In the present article, the rubber compounds are constituted by two well-differentiated phases: vulcanized rubber (SBR) and EPDMd. The interaction between these phases or even between the SBR particles can be very weak, leading to poor mechanical properties and alteration of the dielectric properties by the simple effect of voids inside the blend. To avoid these nondesirable effects, taking advantage of the possibilities offered by the devulcanization of the EPDM, the blends SBR/EPDMd are newly vulcanized. With this approach, the recycling of EPDM achieves the regeneration of a product in its original use, as it were fresh.

To provide insight into the microstructure of the new material derived from the combination of these polymers, electronic microscopy and thermogravimetric analysis (TGA) have been used.[33−35] Another important aspect to consider is the presence of carbon black (CB), which increases the permittivity and promotes the conductivity, some features to take into account when using these materials as dielectrics for capacitors.[36]

The conduction phenomena in polymers are well described by a hopping mechanism;[37−39] the few electrons with high energy levels can move "hopping" from one trap site to another in dielectrics. The activation energy must be understood as the amount of energy that a particle needs to achieve to become a conductor[40] and is a measurement related to the insulation ability of the material.

In this study, we devulcanized EPDM scraps from roof insulating layers. We blended them with the common dielectric elastomers of SBR and studied the microstructure and properties of the resulting revulcanized composites with focus on the dielectric properties for a better understanding of the mechanisms that influence dielectric behavior and the suitability of the resulting materials for electrical applications, looking to expand the possibilities of recycling EPDM waste. Our aim is to provide a wide understanding of the properties in an area. Electrical applications with recycled elastomers are not largely seen nowadays and information on them, except in specific cases,[41−44] is scarce.

2. MATERIALS AND METHODS

Styrene butadiene rubber (SBR) was supplied by VIGAR (Vilafranca del Penedès, Spain). EPDM scraps originally used as the insulation fabric for roofs were provided by Firestone Building Products (Terrassa, Spain). EPDM scraps contain a very relevant presence of carbon black and aluminum silicate. The complete composition is shown in Table 1.

Table 1. Firestone EPDM Building Materials Composition

composition	EDPM	carbon black	aluminum silicate	plasticizer
EPDM scraps	35%	35%	15%	15%

To avoid the effect of carbon black (CB) on the results and aiming to investigate the changes produced by the microstructure of the polymers, the amount of this additive (CB) was kept equal in all samples. This means that the amount of CB included in a sample by incorporating EPDM has been dosed in the others as pure CB, ensuring that the CB content is identical in all samples.

The samples were prepared firstly by inserting the EPDM fabric in a Brabender plastograph (Brabender Gmbh, Duisburg, Germany), where the thermomechanical devulcanization takes place. The material is processed for 3 min. After that, 2 phr of benzoyl peroxide (BPO) is added and the thermomechanical process continues for 20 min. The temperature is set at 80 °C at a speed of 80 rpm. The resulting product is placed into a prototype microwave oven equipped with agitation and is irradiated for 3 min at 700 W. The product obtained after the thermomechanical microwave devulcanization is called EPDMd. The conditions of these treatments have been tested by the authors in previous publications.[17]

After the devulcanization treatment, this EPDMd was blended with SBR in a two-rolls mixing machine, type W 100 T from Dr. Collin GmbH (Germany), by adding carbon black (30 phr) and the sulfur curing system. Further, it was pressed into 3 mm sheets using a Dr. Collin GmbH (Germany) hot plate press for 12 min at a temperature of 160 °C and a pressure of 200 bar. The sheets were then shaped in the test samples according to the dimensions required by the analysis performed.

The curing system composition (phr) was zinc oxide 5.0; stearic acid 3.0; TBBS 1.0; TMTD 0.25; and sulfur 2.0. The same curing system was used for all of the samples.

The thermogravimetric analysis (TGA) of the SBR/EPDMd samples was carried out using TGA/SDTA850e Mettler Toledo equipment. The sample was heated in an N_2 atmosphere from 20 to 800 °C at 20 °C/min and then the sample was kept at 800 °C

https://doi.org/10.1021/acsomega.2c08115
ACS Omega 2023, 8, 12830−12841

Figure 1. (a) Dynamic electric analysis test electrodes with the sample inside. (b) Dynamic electric analysis control parameters of frequency and temperature (Novocontrol unit). (c) Scanning electronic microscopy using JEOL 5610.

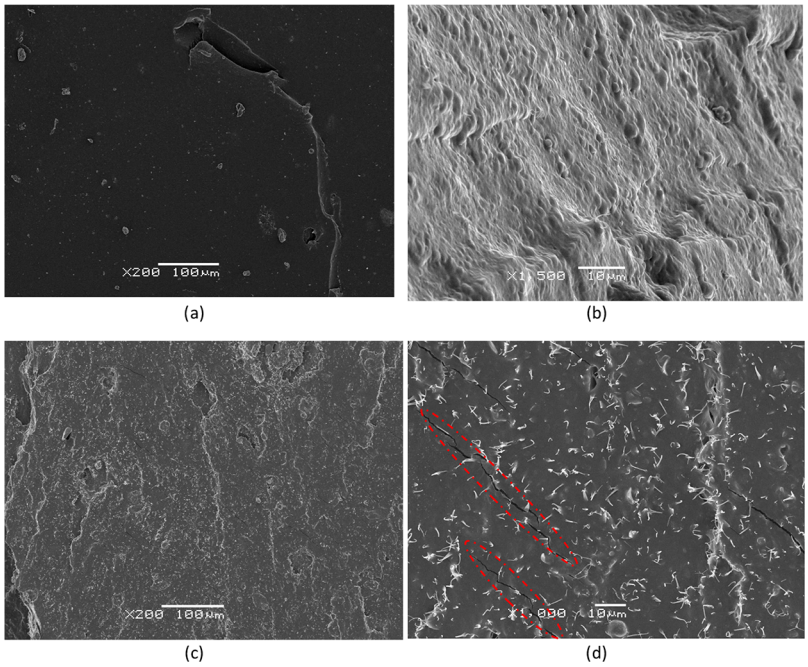

Figure 2. Micrographs of SBR and SBR + 20% EPDMd. (a) SBR at 200 rises; (b) SBR at 1500 magnifications; (c) SBR + 20% EPDMd at 200 augmentations; and (d) SBR + 20% EPDMd at 1000 augmentations.

for 5 min in an oxygen atmosphere (O_2, oxidant), determining the mass loss as a function of temperature.

For the analysis of the microstructure, scanning electron microscopy (SEM) microphotographs were obtained, using a JEOL 5610 microscope (Figure 1c). The samples were previously coated with a thin layer of gold to increase the conductivity. The samples were photographed at magnifications of 200×, 1000×, and 1500×.

The analysis related to the dielectric characterization was carried out using an impedance spectroscopy machine for dynamic electric analysis (DEA) and a novocontrol test equipment (Figure 1b). For this test, a piece of the test sample was cut, with dimensions of 2.5 cm diameter and 0.1 mm thickness, which was placed on the measuring electrodes of the instrument (Figure 1a).

3. RESULTS AND DISCUSSION

3.1. Scanning Electron Microscopy. The SEM micrographs of the EPDMd samples are shown in Figure 2. The analysis of the images reveals changes at a microstructural level. These changes are perceived in the surface of the material as a result of the incorporation of EPDMd material in the form of pores, microcracks, larger cracks, and small holes (Figure 2d,e). On the other hand, the particles of EPDM appear integrated in the matrix; no loose particles in general appear except perhaps for small microagglomerates that may be present, as shown in Figure 2c, which will be discussed later. These two features have influence on the dielectric behavior, because of the voids produced by the micropores or cracks and the interfacial integration produced when two phases are present in the same sample.

3.2. Thermogravimetric Analysis. Figure 3a,b shows the thermogravimetric analysis (TGA) results of samples of EPDMd, SBR, and samples containing 20 and 40% of EPDMd. In this test we can observe the thermodegradation temperatures of the blends that are manifested by a dropping of weight. In this case three regions can be observed. Initially there is a slow decrease of mass that starts over 200 °C and that is related to the volatile compounds present in the polymers and oils, which can decompose around 250 °C. The next region is characterized by a big mass loss centered at 460 °C that corresponds to the decomposition of the elastomers. Finally, the

https://doi.org/10.1021/acsomega.2c08115
ACS Omega 2023, 8, 12830−12841

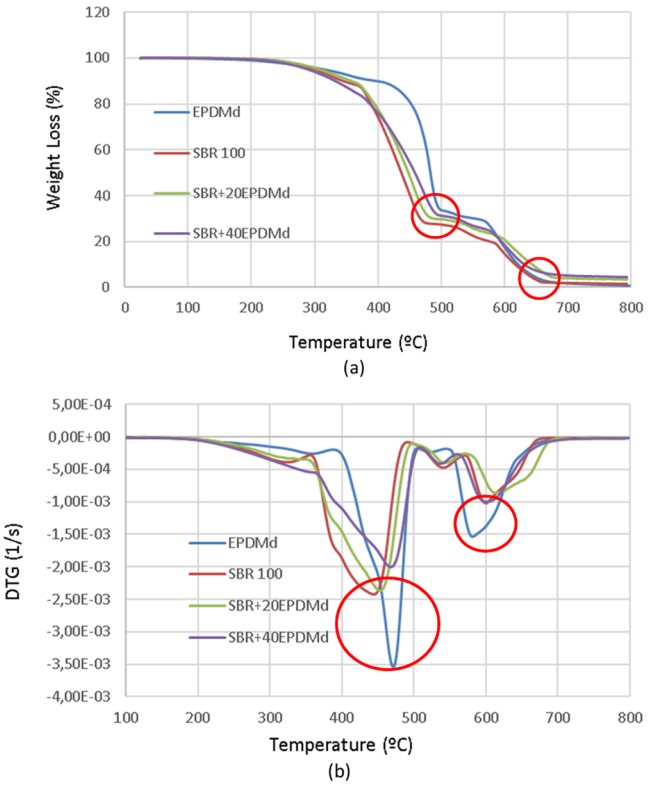

Figure 3. Thermogravimetric analysis (TGA), mass loss versus temperature (°C). (a) Percent of weight loss (%) versus temperature (°C) for EPDMd, SBR, and SBR + EPDMd; (b) derivative thermogravimetry (DTG) (1/*s*) versus temperature (°C) for EPDMd, SBR, and SBR + EPDMd.

next weight loss corresponds to the combustion of carbon black starting at about 600 °C.

On observing the decomposition temperatures in Figure 3 a and more clearly in Figure 3b, we can find a displacement of the decomposition temperatures of every component. The temperatures are marked with a circle in the figures. A shift in these temperatures is associated with the influence of one polymer on the other. This means that adding EPDMd to SBR modifies the decomposition temperature (T_d) to higher values (the T_d of EPDMd is 470 °C) because of the interactions that SBR-EPDMd develop. This indicates the presence of interactions between polymers, which is usually desirable to achieve a good blending and better properties.[18] Since EPDM is more resistant than most elastomers to the temperature and oxidative action combined, the shift when adding EPDM goes to higher temperatures. These results support the observations in SEM, where the EPDMd appeared well integrated in the SBR matrix.

3.3. Real Dielectric Constant—Real Permittivity Part. In Figure 4, the results obtained for the dielectric constant of SBR show a linear behavior with frequency at high frequencies. Temperature increases the dielectric constant by the increase of the polarizability related to the double bonds in the phenyl rings present in SBR. Adding 20% of EPDMd has an important effect on the dielectric constant, increasing it noticeably. The temperature affects less the increase of dielectric constant observed in the case of the neat SBR. Probably the increase in the dielectric value is caused by the additives included in EPDM (Table 1), and also this effect overcomes the affectation by temperature, appearing as less evident in this case. Composites containing 40% EPDMd follow the same trend as those with 20% EPDMd, and the results are in consonance except at low temperatures (30 and 40 °C), where the permittivity reaches lower values than expected from the trend. These results can be attributed to the formation of microagglomerates of EPDMd. When the amount of EPDMd in the sample is relatively high, during the vulcanization process of the samples, EPDM tends to vulcanizate in the form of small clusters, giving preference to the links with other EPDM molecules because of the higher affinity than with SBR.[45] These small microphases are formed by tighter networks, which cause a decrease in polarizability and hence permittivity.

The interactions observed in the TGA may affect the dielectric constant too. When the amount of EPDM is higher, SBR molecules will be involved in secondary bonds with EPDM and that would affect the dielectric values.

Comparing the dielectric constant at low frequencies, there is also an increase of the dielectric constant when adding EPDMd to SBR, as observed before, due to the additives present in EPDMd scraps; aluminum silicate has a higher permittivity than the SBR matrix (AlS = 6.3), and this explains the permittivity rises by the increase of EPMDd content, according to Figure 4a−c, which shows a growing rise of the real permittivity part. The temperature dependence is not so much affected by the presence of EPDMd as in high frequencies and the samples behave similarly lineal with the increase of the temperature.

3.4. Imaginary Permittivity Part. In Figure 5, representative data sets in the frequency domain of the samples at different temperatures are presented. Two types of relaxations are distinguished: α and β. The α relaxation appears at low frequencies and the β relaxation at high frequencies. The α relaxation does not follow Arrhenius temperature behavior and is dependent on the styrene content in the sample. The β relaxation shows an Arrhenius behavior, where the activation energy is independent of the styrene content. As observed by other researchers,[46] the β frequency varies with the temperature (Figure 5a). In Figure 5b,c, corresponding to the composites including EPDMd, no dielectric relaxation peak can be distinguished in the analyzed frequency range (10^{-2} to 3×10^6 Hz). Again, as discussed in the previous section, the presence of aluminum silicate and additives in the EPDMd affects the imaginary permittivity and increases the ε'' value by one magnitude order when comparing Figure 5a−c, so the composites have slightly risen in imaginary permittivity with the EPDMd incorporation. The results obtained for the composition including 40% of EPDMd at low temperatures are also justified by the presence of microagglomerates as explained above.

3.5. Real Part of the Electric Modulus. The electric modulus is the inverse of permittivity, and it is used to analyze the dielectric conduction processes. Figure 6 shows the real part of the electric modulus (M'). Few changes in the three figures analyzed (Figure 6a−c) can be observed. Basically, there is a slight decrease in M' at both low and high frequencies produced by the presence of EPDMd (Figure 6b,c) in the original SBR samples (Figure 6a).

3.6. Imaginary Electric Modulus. The imaginary dielectric modulus is a formalism used to detect dielectric relaxations in the range of frequencies analyzed and is the inverse of imaginary permittivity; at a general level, the M'' behavior decreases slightly with EPDMd content, as is seen in Figure 7. In this case, a rather disparate behavior is seen in the three studied cases. As previously discussed, two relaxations can be observed (Figure 7): the α relaxations, which are located at low frequencies, and

https://doi.org/10.1021/acsomega.2c08115
ACS Omega 2023, 8, 12830−12841

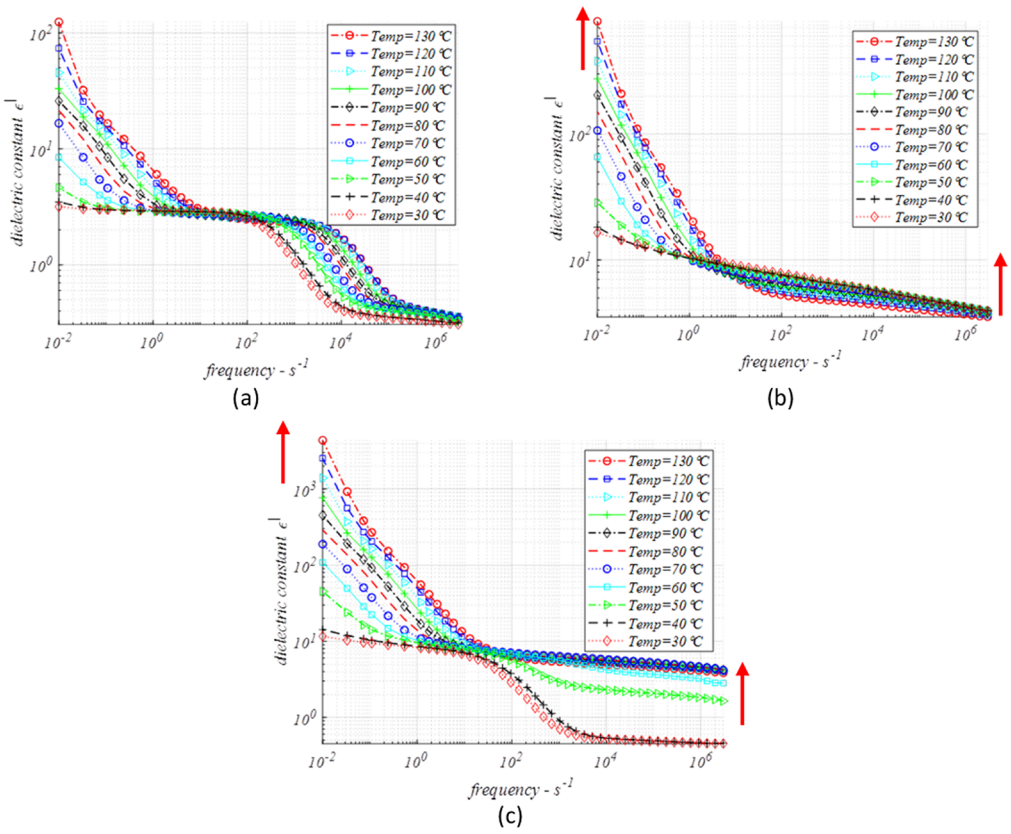

Figure 4. Dielectric constant (ε') versus frequency (Hz) in the temperature dependence (°C) of styrene butadiene rubber (SBR) and SBR-EPDMd composites: (a) SBR 100, (b) SBR + 20% EPDMd, and (c) SBR + 40% EPDMd.

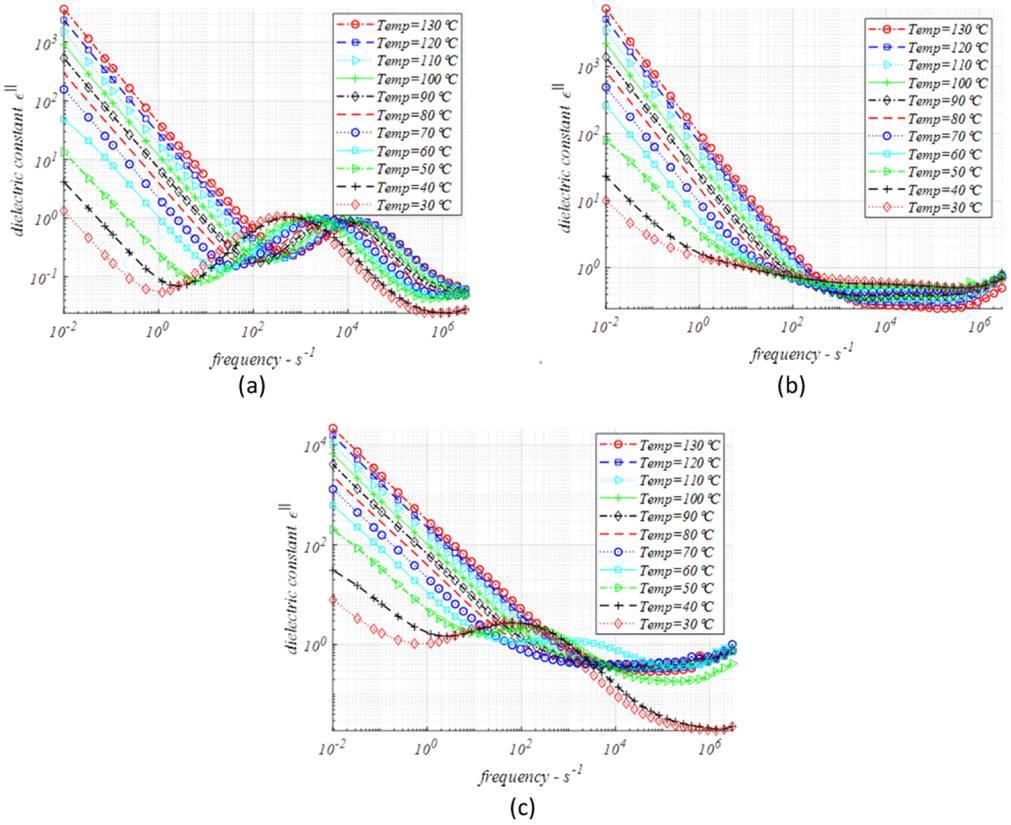

Figure 5. Imaginary permittivity part (ε'') versus frequency (Hz) in the temperature dependence (°C) of styrene butadiene rubber (SBR) and SBR-EPDMd composites: (a) SBR 100, (b) SBR + 20% EPDMd, and (c) SBR + 40% EPDMd.

https://doi.org/10.1021/acsomega.2c08115
ACS Omega 2023, 8, 12830−12841

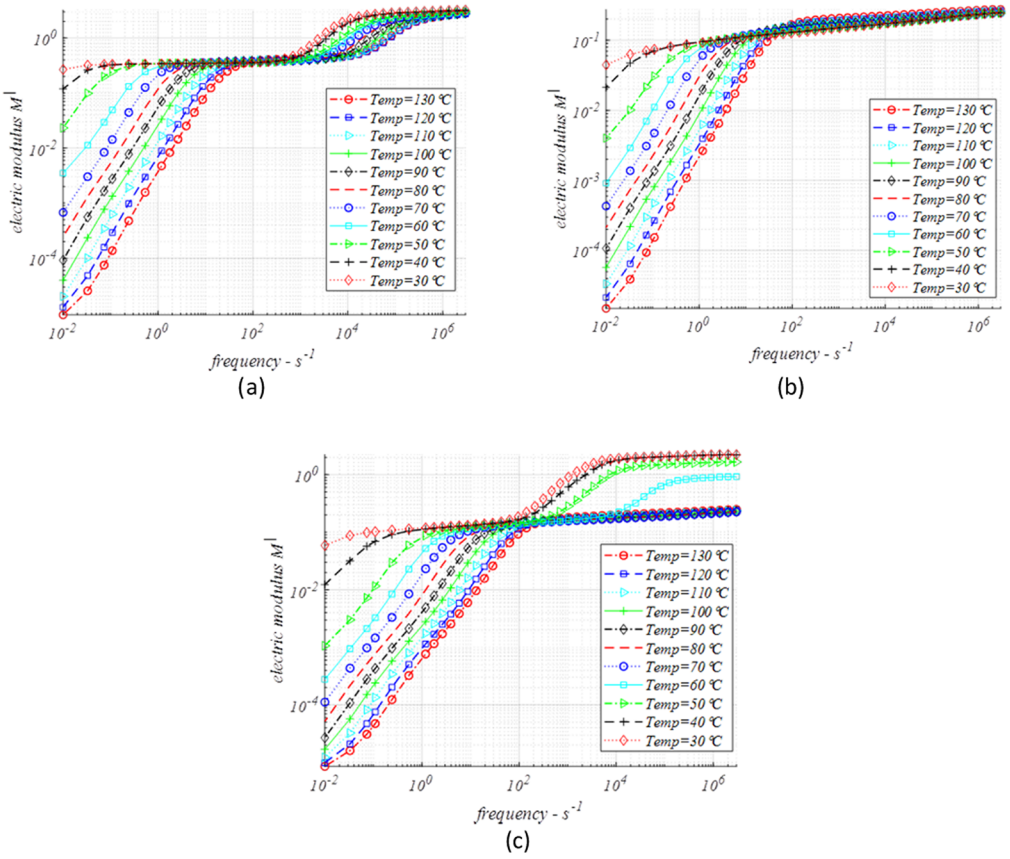

Figure 6. Real part of dielectric modulus (M'') versus frequency (Hz) in the temperature dependence (°C) of styrene butadiene rubber (SBR) and SBR-EPDMd composites: (a) SBR 100, (b) SBR + 20% EPDMd, and (c) SBR + 40% EPDMd.

the β relaxations, which appear at high frequencies. Figure 7a clearly shows both for the SBR material. Both transitions are related to different structures, with α being dependent on the styrene content of the sample and β being independent but related to the local phenomena of the butadiene rubber as described by Cerveny et al.[46]

As shown in Figure 7, the presence of EPDMd affects very clearly the relaxations. When adding EPDMd only α relaxations are observed (Figure 7b,c). The disappearance of the β relaxation may be related to the lower concentration of butadiene rubber present in the samples containing EPDM, but also, more interestingly, to the possible reaction of the butadiene bonds with EPDMd during the curing process. This would indicate that the vulcanization including EPDMd is more effective in the butadiene. This phenomenon can also be observed in Figure 7c. The results when adding a 40% EPDMd define the β transitions when measured at low temperatures. This does not happen when the content of EPDMd is 20%. The increased content of EPDMd to 40%, as explained in previous sections, causes the microagglomerates of EPDMd, which tend to react with their own kind more than with the SBR, leaving some butadiene bonds without reacting, and then the β transition related to butadiene can be observed. Since the β transition is in all cases more visible at lower temperatures, it appears only at temperatures around 60 °C or below that value.

These measurements provide some other important information at the dielectric level. No Maxwell−Wagner−Sillars type relaxations[47] are observed. This relaxation appears when there are two different phases in heterogeneous materials, so it is a very good indicator at a structural level that the composite has had a good integration between its two phases, SBR + EPDMd, corroborating the observations reported of the SEM images presented above.

3.7. Conductivity. Figure 8 presents the DC regime of the conductivity of SBR 100 (Figure 8a), the composite SBR with 20% EPDMd (Figure 8b), and the blend of SBR with 40% EPDMd (Figure 8c). There are clearly different behaviors in the direct (DC) and alternating current regimes of conductivity. In DC the results are very similar in the three studied cases. The conductivity value varies slightly, with the most resistive samples being those made of SBR 100, and then it increases slightly with the presence of EPDMd in the analyzed samples (8b and 8c), although the conductivity changes are not very relevant. The conductivity in the samples with EPDMd (Figure 8b,c) is higher than in SBR; this is due to the aluminum silicate presence in EPDMd fraction's samples. As discussed previously, the addition of EPDMd scraps and devulcanized particles implies addition of aluminum silicates, plasticizers, and other additives, which are more conductive than the SBR matrix. This causes two effects: an increase of the conductivity of the SBR/EPDMd composites (Figure 8b,c) and the increase of the conductivity in the DC regime.

3.8. Cole−Cole Diagram. The Cole−Cole diagram presents a graph, $\varepsilon''-\varepsilon'$, of the various materials analyzed. In Figure 9a the SBR without additives presents a Debye-like behavior at low frequencies,[48] between 10^{-1} and $10^{0.2}$ Hz. This has been deduced from the semicircle observed in this frequency range, in a very similar way for all temperatures analyzed. From here, the presence of devulcanized EPDM (Figure 9b,c) modifies this behavior, showing non-Debye behavior[49] also for

https://doi.org/10.1021/acsomega.2c08115
ACS Omega 2023, 8, 12830−12841

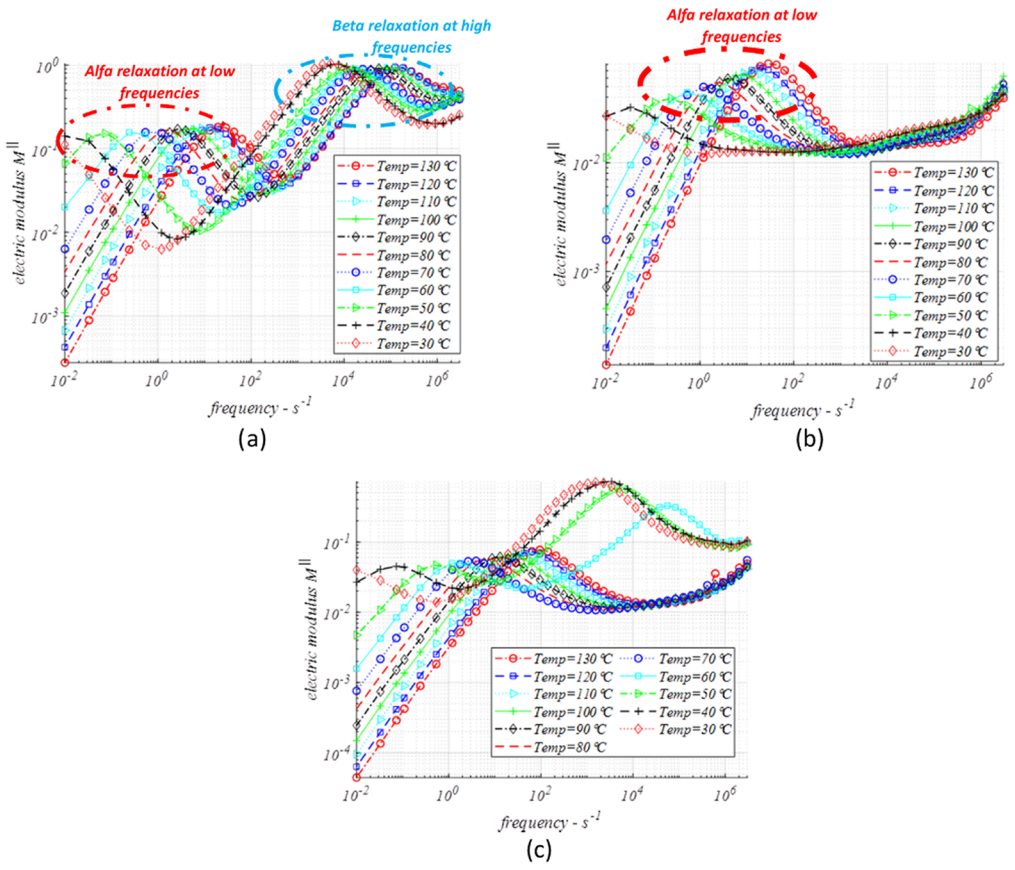

Figure 7. Real part of dielectric modulus (M') versus frequency (Hz) in the temperature dependence (°C) of styrene butadiene rubber (SBR) and SBR-EPDMd composites: (a) SBR 100, (b) SBR + 20% EPDMd, and (c) SBR + 40% EPDMd.

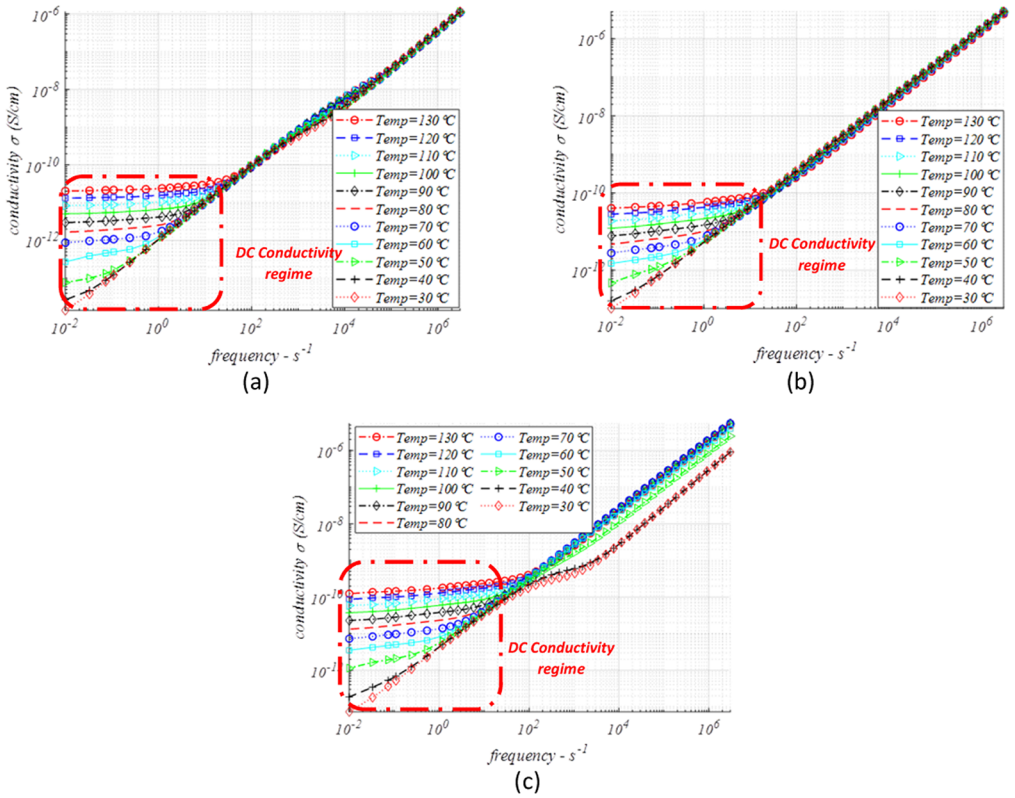

Figure 8. Conductivity (σ) versus frequency (Hz) in the temperature dependence (°C) of styrene butadiene rubber (SBR) and SBR-EPDMd composites: (a) SBR 100, (b) SBR + 20% EPDMd, and (c) SBR + 40% EPDMd.

https://doi.org/10.1021/acsomega.2c08115
ACS Omega 2023, 8, 12830−12841

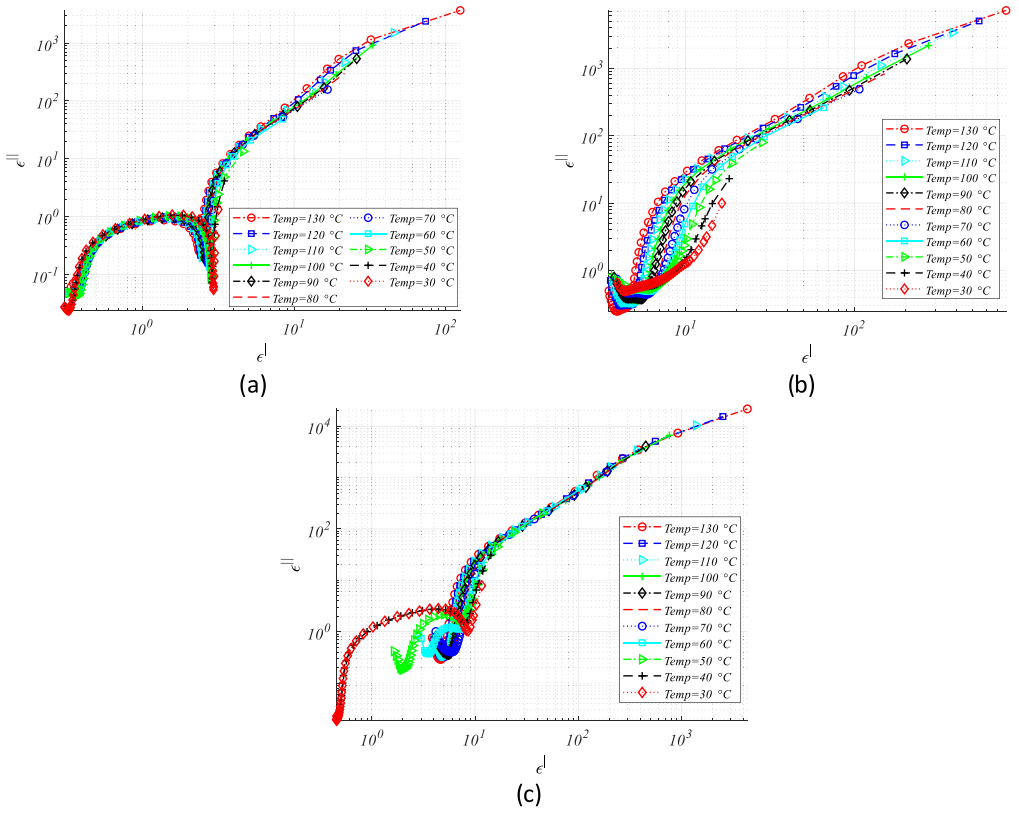

Figure 9. Cole−Cole diagram in the temperature dependence (°C) of styrene butadiene rubber (SBR) and SBR-EPDMd composites: (a) SBR 100, (b) SBR + 20% EPDMd, and (c) SBR + 40% EPDMd.

low and high frequencies. In this case, there is an absence of similar figures to the semicircles in each of the last two figures (Figure 9b,c). This indicates that the composites SBR-EPDMd do not produce a compound with a macrodipole behavior, so the electrical structure does not have a macroelectrode or macrodipole dielectric behavior and does not allow the passage of low conductive loads under the electric field applied at all temperature ranges analyzed. The macrodipole concept has been elaborated in the next section.

3.9. Argand Diagram. Argand diagram is the representation of the impedance in a vector diagram through the electric modulus representation. The impedance of the material can be considered as a vector magnitude and is represented in a vector diagram or Argand diagram by employing a point. Each point represents the magnitude and direction of the electric modulus vector at a given frequency. This way of displaying complex impedance as a function of frequency is known as an Argand diagram. Coelho's space charge contribution theory[50,51] is based on the macroscopic dipole concept. An electrically neutral sample has mobile carriers uniformly distributed in the absence of a field. If an electric field is applied to the sample, the mobile carriers move toward the electrode of the opposite sign, leaving carriers of the opposite sign next to the other electrode, resulting in the following charge distribution once equilibrium is reached. This distribution constitutes a macrodipole that would oscillate in an alternating field with the frequency of the field, causing a relaxation process that affects the heat of the medium's permittivity. To deduce the Argand diagram, the electric modulus is represented in Figure 10: M'' or the imaginary part of the electric modulus versus M′ or the real part of the electric modulus. For a macrodipole behavior to occur, semicircles should be drawn in the representation of the Argand and Cole−Cole diagrams, which does not happen, so it is considered that these materials at the dielectric level have a non-Debye behavior.

3.10. Activation Energies. The activation energy is the minimum energy needed for a certain process to occur;[52] in this case, we are considering the conduction of electrons, and therefore that this medium or material becomes conductive. The activation energy of a reaction is usually denoted by E_a. The activation energy can be considered as the height of the potential barrier (called the energy barrier) that separates two minima of potential energy (of the reactants and products of a reaction). To establish this correlation, the following equation is used.

$$\sigma_{dc} = \sigma_0 \cdot e^{(-E_a/k_B \cdot T)}$$

where the variables are σ_{dc}: the conductivity value in the DC regime, observed in Figure 6; σ_0: this value is comparable to 1; E_a: the activation energy we are looking for and expressed in electron volts (eV); it represents the energy necessary to activate conduction processes in these materials; k_B: Boltzmann constant; e: the exponential number e; T: the temperature in Kelvins to which the process is subjected; in the present experiment it varies from 303 to 403 K, so there is a 100 K temperature difference from the minimum to the maximum. The data shown indicate that for pure SBR the activation energy (E_a) is 0.79 eV and that with the incorporation of 20% of devulcanized EPDM the E_a drops to 0.65 eV, and with the increase of EPDMd up to 40% the activation energy increases to 0.77 eV, according to Figure 11. The presence of aluminum silicates in the SBR + EPDMd samples causes the activation energies to decrease, and it requires less energy to increase the conduction processes in the composite samples of SBR +

https://doi.org/10.1021/acsomega.2c08115
ACS Omega 2023, 8, 12830−12841

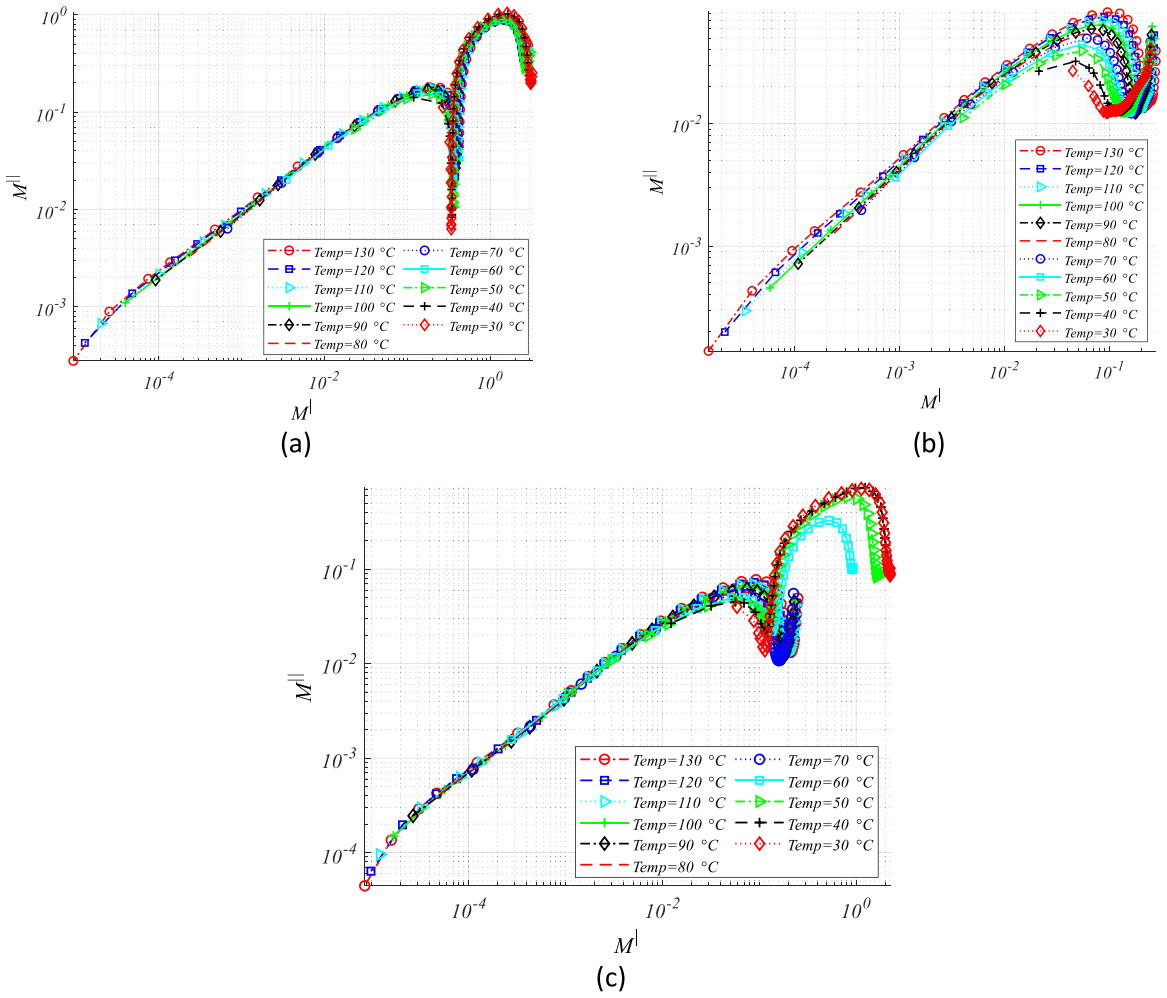

Figure 10. Argand diagram for the temperature dependence (°C) of styrene butadiene rubber (SBR) and SBR-EPDMd composites: (a) SBR 100, (b) SBR + 20% EPDMd, and (c) SBR + 40% EPDMd.

EPDMd, which also, therefore, worsens the quality of the dielectric insulation.

4. CONCLUSIONS

The main conclusions of the present research are that the addition of devulcanized EPDM to an SBR rubber matrix maintains a certain electrical insulating behavior, although it slightly increases the composite conductivity and permittivity. Thermally, it presents a similar behavior in the three analyzed samples: SBR; SBR + 20% EPDMd; and SBR + 40% EPDMd. There are, however, remarkable facts that are relevant and worth noting about the changes observed and they are the following:

1. At a structural level, it is observed that the EPDMd phase integrates very well into the SBR matrix, according to the SEM analysis. This is consequent to the fact that no Maxwell−Wagner−Sillars type relaxations are observed.
2. At the dielectric level, in the frequency-dependent analysis, α relaxations are observed at low frequencies and β relaxations at high frequencies (dependent on the presence of butadiene in the sample);[53] the presence of EPDMd means that β relaxations are imperceptible in the analyzed frequency range.
3. The samples have non-Debye dielectric behavior. This implies that they do not have macrodipole behavior, a fact observed in a large part of the composites analyzed dielectrically.
4. The activation energies, in this case, are also affected by the presence of EPDMd, with less energy being needed to activate the conduction processes in the analyzed compounds.
5. The dielectric features analyzed, mainly permittivity and conductivity, slightly enhance the values from the measured properties due to the presence of aluminum silicate in the EPDMd matrix, which leads to SBR/EPDMd composites with higher levels of conductivity and permittivity, slightly damaging the insulation behavior of the original SBR.
6. At the level of dielectric application, these are not materials with high permittivity, so they would not be good insulators for capacitors, but they do have a certain electrical resistance at low frequencies and hence could be used for electrical roofs or as low-voltage insulators.[54]

AUTHOR INFORMATION

Corresponding Author

Marc Marín-Genescà − *Department of Mechanical Engineering, ETSEQ-URV, 45002 Tarragona, Spain;* orcid.org/0000-0002-7204-4526; Email: marc.marin@urv.cat

https://doi.org/10.1021/acsomega.2c08115
ACS Omega 2023, 8, 12830−12841

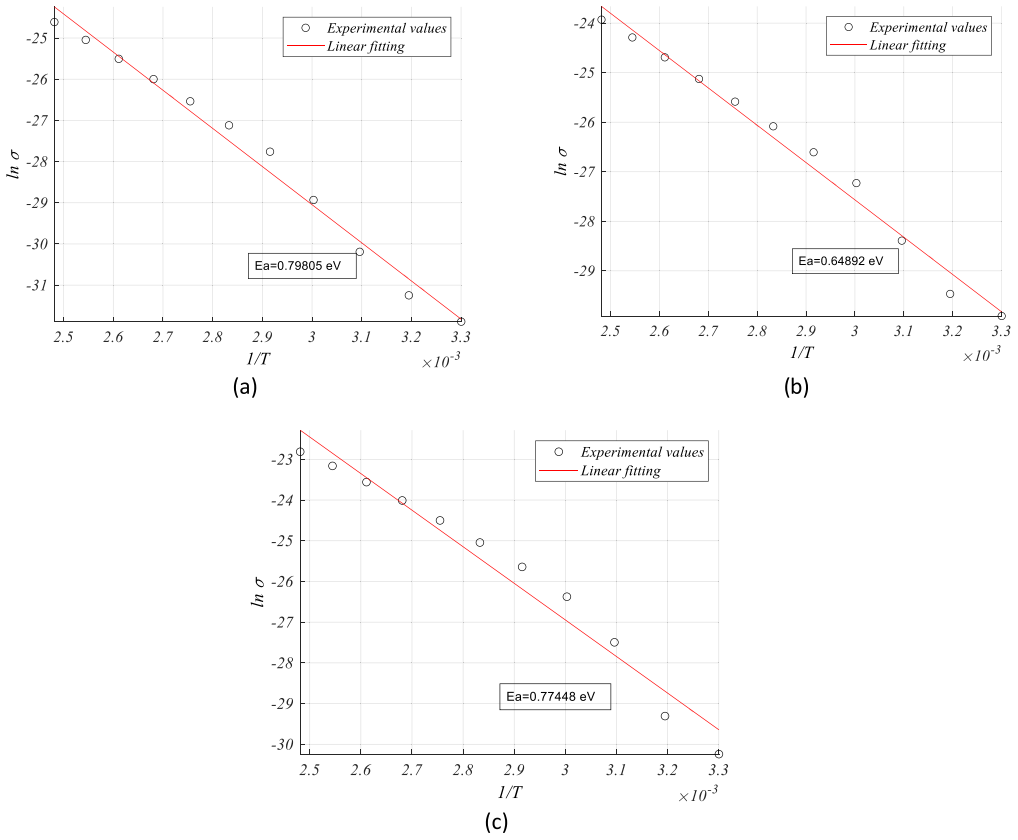

Figure 11. Activation energy (eV) of styrene butadiene rubber (SBR) and SBR-EPDMd composites: (a) SBR 100, (b) SBR + 20% EPDMd, and (c) SBR + 40% EPDMd.

Authors

Jordi García-Amorós − *Department of Electrical Engineering, ETSE-URV, 45002 Tarragona, Spain*

Miguel Mudarra − *Department of Physics Applied, ESEIAAT-UPC, 08222 Terrassa, Spain*

Lluis Massagués Vidal − *Department of Electrical Engineering, ETSE-URV, 45002 Tarragona, Spain*

Javier Cañavate − *Department of Chemical Engineering, ESEIAAT-UPC, 08222 Terrassa, Spain*

Xavier Colom − *Department of Chemical Engineering, ESEIAAT-UPC, 08222 Terrassa, Spain*

Complete contact information is available at: https://pubs.acs.org/10.1021/acsomega.2c08115

Notes

The authors declare no competing financial interest.

■ ACKNOWLEDGMENTS

The authors wish to acknowledge the support of the next research groups to this research: Greeli—Grup de Recerca d'Enginyeria Elèctrica i Instrumentació from URV University and Polquitex and DILAB—Laboratori de física dels materials dielèctrics from UPC University. The authors thank the financial support from Ministerio de Ciencia e Innovación, project reference PID2021-126165OB-I00, corresponding to the 2021 call for Knowledge Generation Projects 2021.

■ REFERENCES

(1) Sutanto, P.; Picchioni, F.; Janssen, L. P. B. M.; Dijkhuis, K. A. J.; Dierkes, W. K.; Noordermeer, J. W. M. State of the Art: Recycling of EPDM Rubber Vulcanizates. *Int. Polym. Process.* **2006**, *21*, 211−217.

(2) *Handbook of Elastomers*, 2nd ed.; Bhowmick, A. K.; Stephens, H., Eds.; CRC Press, 2001.

(3) Botros, S. H.; Tawfic, M. L. Preparation and Characteristics of EPDM/NBR Rubber Blends with BIIR as Compatibilizer. *Polym.-Plast. Technol. Eng.* **2005**, *44*, 209−227.

(4) Mat, N. S. C.; Ismail, H.; Othman, N. Curing Characteristics and Tear Properties of Bentonite Filled Ethylene Propylene Diene (EPDM) Rubber Composites. *Procedia Chem.* **2016**, *19*, 394−400.

(5) Prut, E.; Erina, N.; Karger-Kocsis, J.; Medintseva, T. Effects of blend composition and dynamic vulcanization on the morphology and dynamic viscoelastic properties of PP/EPDM blends. *J. Appl. Polym. Sci.* **2008**, *109*, 1212−1220.

(6) Baldwin, F. P.; Borzel, P.; Cohen, C. A.; Makowski, H. S.; Van de Castle, J. F. The Influence of Residual Olefin Structure on EPDM Vulcanization. *Rubber Chem. Technol.* **1970**, *43*, 522−548.

(7) Jacob, C.; De, P. P.; Bhowmick, A. K.; De, S. K. Recycling of EPDM waste. I. Effect of ground EPDM vulcanizate on properties of EPDM rubber. *J. Appl. Polym. Sci.* **2001**, *82*, 3293−3303.

(8) Movahed, S. O.; Ansarifar, A.; Karbalaee, S.; Far, S. A. Devulcanization and Recycling of Waste Automotive Epdm Rubber Powder by Using Shearing Action and Chemical Additive. *Prog. Rubber, Plast. Recycl. Technol.* **2015**, *31*, 87−116.

(9) Mohaved, S. O.; Ansarifar, A.; Nezhad, S. K.; Atharyfar, S. A novel industrial technique for recycling ethylene-propylene-diene waste rubber. *Polym. Degrad. Stab.* **2015**, *111*, 114−123.

(10) Fukumori, K.; Matsushita, M.; Okamoto, H.; Sato, N.; Suzuki, Y.; Takeuchi, K. Recycling technology of tire rubber. *JSAE Rev.* **2002**, *23*, 259−264.

(11) Hassanpour-Kasanagh, S.; Ahmedzade, P.; Fainleib, A. M.; Behnood, A. Rheological properties of asphalt binders modified with recycled materials: A comparison with Styrene-Butadiene-Styrene (SBS). *Constr. Build. Mater.* **2020**, *230*, No. 117047.

(12) Jacob, C.; Bhowmick, A. K.; De, P. P.; De, S. K. Utilization of Powdered EPDM Scrap in EPDM Compound. *Rubber Chem. Technol.* **2003**, *76*, 36−59.
(13) Pirityi, D. Z.; Pölöskei, K. Thermomechanical Devulcanisation of Ethylene Propylene Diene Monomer (EPDM) Rubber and Its Subsequent Reintegration into Virgin Rubber. *Polymers* **2021**, *13*, 1116.
(14) Liang, H.; Hardy, J.-M.; Rodrigue, D.; Brisson, J. EPDM Recycled rubber powder characterization: thermal and thermogravimetric analysis. *Rubber Chem. Technol.* **2014**, *87*, 538−556.
(15) Zedler, Ł.; Colom, X.; Cañavate, J.; Saeb, M. R.; T Haponiuk, J.; Formela, K. Investigating the Impact of Curing System on Structure-Property Relationship of Natural Rubber Modified with Brewery By-Product and Ground Tire Rubber. *Polymers* **2020**, *12*, 545.
(16) Zedler, Ł.; Kowalkowska-Zedler, D.; Vahabi, H.; Saeb, M. R.; Colom, X.; Cañavate, J.; Wang, S.; Formela, K. Preliminary Investigation on Auto-Thermal Extrusion of Ground Tire Rubber. *Materials* **2019**, *12*, 2090.
(17) Colom, X.; Cañavate, J.; Formela, K.; Shadman, A.; Saeb, M. R. Assessment of the devulcanization process of EPDM waste from roofing systems by combined thermomechanical/microwave procedures. *Polym. Degrad. Stab.* **2021**, *183*, No. 109450.
(18) Cañavate, J.; Carrillo, F.; Casas, P.; Colom, X.; Suñol, J. J. The Use of Waxes and Wetting Additives to Improve Compatibility Between HDPE and Ground Tyre Rubber. *J. Compos. Mater.* **2010**, *44*, 1233−1245.
(19) Seghar, S.; Asaro, L.; Rolland-Monnet, M.; Hocine, N. A. Thermo-mechanical devulcanization and recycling of rubber industry waste. *Resour., Conserv. Recycl.* **2019**, *144*, 180−186.
(20) Meysami, M.; Tzoganakis, C.; Mutyala, P.; Zhu, S. H.; Bulsari, M. Devulcanization of Scrap Tire Rubber with Supercritical CO2: A Study of the Effects of Process Parameters on the Properties of Devulcanized Rubber. *Int. Polym. Process.* **2017**, *32*, 183−193.
(21) Kummali, M. M.; Miccio, L. A.; Schwartz, G. A.; Alegría, A.; Colmenero, J.; Otegui, J.; Petzold, A.; Westermann, S. Local mechanical and dielectric behavior of the interacting polymer layer in silica nanoparticles filled SBR through AFM-based methods. *Polymer* **2013**, *54*, 4980−4986.
(22) Renukappa, N. M.; Siddaramaiah; Sudhaker Samuel, R. D.; Sundara Rajan, J.; Lee, J. H. Dielectric properties of carbon black: SBR composites. *J. Mater. Sci.: Mater. Electron.* **2009**, *20*, 648−656.
(23) John, H.; Joseph, R.; Mathew, K. T. Dielectric behavior of natural rubber composites in microwave fields. *J. Appl. Polym. Sci.* **2007**, *103*, 2682−2686.
(24) Hernández, M.; Bernal, M. d. M.; Verdejo, R.; Ezquerra, T. A.; López-Manchado, M. A. Overall performance of natural rubber/graphene nanocomposites. *Compos. Sci. Technol.* **2012**, *73*, 40−46.
(25) Van Beek, L. K. H. The Maxwell-Wagner-Sillars effect, describing apparent dielectric loss in inhomogeneous media. *Physica* **1960**, *26*, 66−68.
(26) McKenzie, R.; Zurawsky, W.; Mijovic, J. A molecular interpretation of Maxwell−Wagner−Sillars processes. *J. Non-Cryst. Solids* **2014**, *406*, 11−21.
(27) Constantino, G. A program for the fitting of Debye, Cole−Cole, Cole−Davidson, and Havriliak−Negami dispersions to dielectric data. *J. Colloid Interface Sci.* **2014**, *419*, 102−106.
(28) Iglesias, T. P.; Vilão, G.; Reis, J. C. R. An approach to the interpretation of Cole−Davidson and Cole−Cole dielectric functions. *J. Appl. Phys.* **2017**, *122*, No. 074102.
(29) Dotson, T. C.; Budzien, J.; McCoy, J. D.; Adolf, D. B. Cole−Davidson dynamics of simple chain models. *J. Chem. Phys.* **2009**, *130*, No. 024903.
(30) Jonscher, A. K. Nature (London). *J. Phys. D: Appl. Phys.* **1999**, *32*, No. R57.
(31) Jonscher, A. K. A new understanding of the dielectric relaxation of solids. *J. Mater. Sci.* **1981**, *16*, 2037−2060.
(32) Cole, R. H. On the Analysis of Dielectric Relaxation Measurements. *J. Chem. Phys.* **1955**, *23*, 493−499.
(33) Stefani, P. M.; Garcia, D.; Lopez, J.; Jimenez, A. Thermogravimetric analysis of composites obtained from sintering of rice husk-scrap tire mixtures. *J. Therm. Anal. Calorim.* **2005**, *81*, 315−320.
(34) Mujal-Rosas, R.; Marin-Genesca, M.; Orrit-Prat, J.; Rahhali, A.; Colom-Fajula, X. Dielectric, mechanical, and thermal characterization of high-density polyethylene composites with ground tire rubber. *J. Thermoplast. Compos. Mater.* **2012**, *25*, 537−559.
(35) Mujal-Rosas, R.; Orrit-Prat, J.; Ramis-Juan, X.; Marin-Genesca, M. Electrical application of polyamide reinforced with old tire rubber (ground tire rubber): Dielectric, thermal, mechanical, and structural properties. *J. Thermoplast. Compos. Mater.* **2014**, *27*, 1209−1231.
(36) Marín-Genescà, M.; García-Amorós, J.; Mujal-Rosas, R.; Massagués Vidal, L.; Colom Fajula, X. Application Properties Analysis as a Dielectric Capacitor of End-of-Life Tire-Reinforced HDPE. *Polymers* **2020**, *12*, 2675.
(37) Carley Read, R. E.; Stow, C. D. An experimental investigation of charge transport through rubber. *J. Phys. D: Appl. Phys.* **1969**, *2*, No. 567.
(38) Ladhar, A.; Arous, M.; Kaddami, H.; Raihane, M.; Kallel, A.; Graça, M. P. F.; Costa, L. C. Ionic hopping conductivity in potential batteries separator based on natural rubber−nanocellulose green nanocomposites. *J. Mol. Liq.* **2015**, *211*, 792−802.
(39) Silva, M. J. d.; Sanches, A. O.; Malmonge, L. F.; Malmonge, J. A. Electrical, mechanical, and thermal analysis of natural rubber/polyaniline-DBSA composite. *Mater. Res.* **2014**, *17*, 59−63.
(40) Deuri, A. S.; Bhowmick, A. K. Aging of EPDM rubber. *J. Appl. Polym. Sci.* **1987**, *34*, 2205−2222.
(41) El-Nashar, D. The compatibilization of EPDM/SBR blends by EMM-graft-styrene copolymer. Polymer-plastics Technology and Engineering. *Polym.-Plast. Technol. Eng.* **2005**, *43*, 1425−1441.
(42) Bahadar, A.; Zwawi, M. Development of SWCNTs-reinforced EPDM/SBR matrices for shock absorbing applications. *Mater. Res. Express* **2020**, *7*, No. 025310.
(43) Saad, A. L. G.; El-Sabbagh, S. Compatibility studies on some polymer blend systems by electrical and mechanical techniques. *J. Appl. Polym. Sci.* **2001**, *79*, 60−71.
(44) Li, B.; Polizos, G.; Manias, E. Interfacial Effects on the Dielectric Properties of Elastomer Composites and Nanocomposites. In *Dynamics of Composite Materials*, Schönhals, A.; Szymoniak, P., Eds.; Advances in Dielectrics; Springer: Cham, 2022.
(45) Goharpey, F.; Katbab, A. A.; Nazockdast, H. Formation of Rubber Particle Agglomerates During Morphology Development in Dynamically Crosslinked EPDM/PP Thermoplastic Elastomers. Part 1: Effects of Processing and Polymer Structural Parameters. *Rubber Chem. Technol.* **2003**, *76*, 239−252.
(46) Cerveny, S.; Bergman, R.; Schwartz, G. A.; Jacobsson, P. Dielectric α- and β Relaxations in Uncured Styrene Butadiene Rubber. *Macromolecules* **2002**, *35*, 4337−4342.
(47) Xia, X.; Zhong, Z.; Weng, G. J. Maxwell−Wagner−Sillars mechanism in the frequency dependence of electrical conductivity and dielectric permittivity of graphene-polymer nanocomposites. *Mech. Mater.* **2017**, *109*, 42−50.
(48) Marín-Genescà, M.; Mujal Rosas, R.; García Amorós, J.; Massagues Vidal, L.; Colom Fajula, X. Influence of Tire Rubber Particles Addition in Different Branching Degrees Polyethylene Matrix Composites on Physical and Structural Behavior. *Polymers* **2021**, *13*, 3213.
(49) Marín-Genescà, M.; García-Amorós, J.; Mujal-Rosas, R.; Massagués, L.; Colom, X. Study, and Characterization of the Dielectric Behavior of Low Linear Density Polyethylene Composites Mixed with Ground Tire Rubber Particles. *Polymers* **2020**, *12*, 1075.
(50) Coelho, R. Sur la relaxation d'une charge d'espace. *Rev. Phys. Appl.* **1983**, *18*, 137−146.
(51) Mudarra, M.; Díaz-Calleja, R.; Belana, J.; Cañadas, J. C.; Diego, J. A.; Sellarès, J.; Sanchís, M. J. Study of space charge relaxation in PMMA at high temperatures by dynamic electrical analysis. *Polymer* **2001**, *42*, 1647−1651.
(52) Mujal-Rosas, R.; Orrit-Prat, J.; Ramis-Juan, X.; Marin-Genesca, M.; Rahhali, A. Study on dielectric, thermal, and mechanical properties

https://doi.org/10.1021/acsomega.2c08115
ACS Omega 2023, 8, 12830−12841

of the ethylene vinyl acetate reinforced with ground tire rubber. *J. Reinf. Plast. Compos.* **2011**, *30*, 581−592.
(53) Ortega, L.; Cerveny, S.; Sill, C.; Isitman, N. A.; Rodriguez-Garraza, A. L.; Meyer, M.; Westermann, S.; Schwartz, G. A. The effect of vulcanization additives on the dielectric response of styrene-butadiene rubber compounds. *Polymer* **2019**, *172*, 205−212.
(54) Marín-Genescà, M.; García-Amorós, J.; Mujal-Rosas, R.; Vidal, L. M.; Arroyo, J. B.; Fajula, X. C. Ground Tire Rubber Recycling in Applications as Insulators in Polymeric Compounds, According to Spanish UNE Standards. *Recycling* **2020**, *5*, 16.

https://doi.org/10.1021/acsomega.2c08115
ACS Omega 2023, 8, 12830−12841